Molecular Beacons

DOI: 10.1002/anie.201209440

DNA Micelle Flares for Intracellular mRNA Imaging and Gene Therapy**

Tao Chen, Cuichen Sam Wu, Elizabeth Jimenez, Zhi Zhu, Joshua G. Dajac, Mingxu You, Da Han, Xiaobing Zhang, and Weihong Tan**

The hybridization between a nucleic acid strand and its complementary sequence, one of the strongest and most specific molecular recognition events,[1] has greatly facilitated the development of disease diagnosis and gene therapy. For example, both linear[2] and hairpin[3] nucleic acid probes have been used to visualize and detect specific messenger RNAs (mRNAs) in living cells. Many mRNAs are disease-related and can be used as specific biomarkers to assess the stage of these diseases, including cancer. Through molecular engineering, these probes can effectively translate an mRNA binding event into a fluorescence signal change without the need to remove unbound free probes. In addition, most human diseases, including cancer, could be treated with the introduction of genetic materials—plasmid DNAs,[4] antisense oligonucleotides,[5] small interfering RNAs,[6] small hairpin RNAs,[7] and microRNAs[8]—into somatic tissues. These genetic materials can either enhance gene expression[9] or inhibit the production of deleterious proteins, thus making nucleic acid probes excellent candidates for gene therapy.[5a] The advantages of nucleic acid probes lie in the simplicity of their synthesis, the suitability of their modification, and the selectivity of their binding.[1b]

However, their potential has not been fully realized because of the following reasons. First, as negatively charged hydrophilic biomacromolecules, nucleic acid probes cannot freely traverse the cell membrane,[10] thus requiring additional instruments (such as microinjection or electroporation) or materials (such as transfection reagents, including cationic lipids/polymers and nanomaterials) for efficient cellular internalization.[5b] Second, nucleic acid probes can be unstable even after successful cellular delivery because of endogenous nuclease digestion,[11] leading to high false positive signals or decreased therapeutic efficiency. Third, most applications for nucleic acid probes focus on either mRNA detection or gene therapy, while a better strategy to improve the patient outcome would be the combination of mRNA imaging[3c,12] and gene therapy[13] into one biomolecular method. Through mRNA imaging, real-time spatiotemporal evaluation of nucleic acid probe delivery and target gene expression can be realized non-invasively, providing useful information for assessing therapeutic efficiency, adjusting treatment methods, and refining probe design.[14] Even though nucleic acid functionalized gold nanoparticles (AuNPs) with efficient cellular uptake[15] and enhanced enzymatic stability[16] have been developed to solve the first two challenges, they suffer non-negligible cytotoxicity at relatively high concentrations as a result of AuNP incorporation.[17] In addition, the preparation of these probes is very time-consuming, requiring more than 24 hours even after obtaining the AuNPs and nucleic acids.[5b] Therefore, an ideal nucleic acid probe should be easy to synthesize, capable of self-delivery, highly biocompatible, and sufficiently stable in a cellular environment, while at the same time, performing multiple functions in living cells.

Herein, we present a sensitive and selective approach for combined mRNA detection and gene therapy using molecular beacon micelle flares (MBMFs). MBMFs are easily prepared by self-assembly of diacyllipid–molecular-beacon conjugates (L-MBs), not requiring any biohazardous materials. Just like pyrotechnic flares that produce brilliant light when activated, MBMFs undergo a significant burst of fluorescence enhancement upon target binding. This hybridization event subsequently induces gene silencing, leading to

[*] T. Chen, C. S. Wu, E. Jimenez, J. G. Dajac, Dr. M. You, D. Han, Prof. Dr. W. Tan
Center for Research at Bio/Nano Interface, Department of Chemistry and Department of Physiology and Functional Genomics, Shands Cancer Center, UF Genetics Institute and McKnight Brain Institute, University of Florida
Gainesville, FL 32611-7200 (USA)
E-mail: tan@chem.ufl.edu
Prof. Dr. X. Zhang, Prof. Dr. W. Tan
Molecular Science and Biomedicine Laboratory, State Key Laboratory of Chemo/Biosensing and Chemometrics, College of Biology and College of Chemistry and Chemical Engineering, Hunan University
Changsha 410082 (P.R. China)
E-mail: xbzhang@hnu.edu.cn
Prof. Dr. Z. Zhu
State Key Laboratory for Physical Chemistry of Solid Surfaces, The Key Laboratory for Chemical Biology of Fujian Province and Department of Chemical Biology, College of Chemistry and Chemical Engineering, Xiamen University
Xiamen 361005 (P.R. China)

[**] This work is supported by grants awarded by the National Institutes of Health (GM066137 and GM079359), and by the National Key Scientific Program of China (2011CB911000), the Foundation for Innovative Research Groups of NSFC (Grant 21221003), China National Instrumentation Program 2011YQ03012412. We thank Dr. Haipeng Liu and Dr. Ruowen Wang for their help on diacyllipid phosphoramidite synthesis, Dr. Craig G. Moneypenny and Dr. Neal A. Benson for their technical assistance with confocal-laser scanning microscopy and flow cytometry, and Dr. Kathryn Williams for her critical comments on the preparation of this manuscript.

Supporting information for this article (experimental details) is available on the WWW under http://dx.doi.org/10.1002/anie.201209440.

apoptosis of cancer cells. The advantages of MBMFs include easy probe synthesis, efficient cellular uptake, enhanced enzymatic stability, high signal-to-background (S/B) ratio, excellent target selectivity, and superior biocompatibility. In this approach (Scheme 1), L-MBs spontaneously self-assemble into MBMFs with a diacyllipid core and an MB corona in

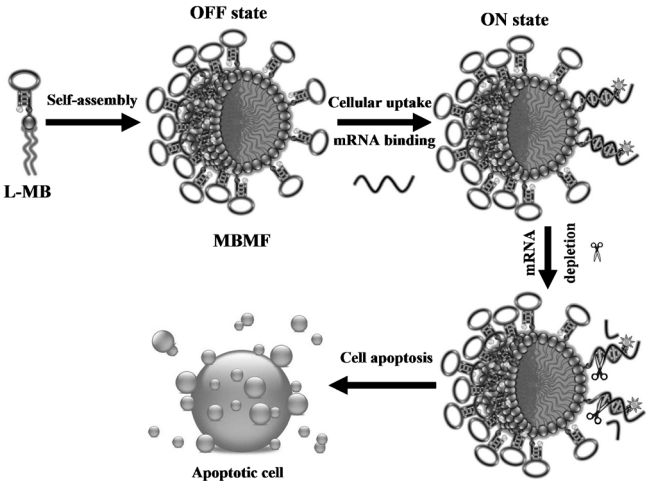

Scheme 1. Schematic illustration of molecular beacon micelle flares (MBMFs) for intracellular mRNA detection and gene therapy. Diacyllipid–molecular-beacon conjugates (L-MBs) self-assemble into MBMFs and enter living cells. Before binding their target mRNA, the fluorophore and the quencher of the MBMFs are in close proximity (OFF state). Hybridization between the loop region and the target mRNA separates the fluorophore and the quencher, producing a fluorescence signal (ON state) and DNA/RNA heteroduplex for RNase H action. Note: not all MBs are shown on the MBMF.

aqueous solutions owing to hydrophobic interactions. The MB part is a DNA sequence composed of a target-recognition loop flanked by two short complementary stem sequences. The formation of the stem-loop (hairpin) structure brings the quencher and fluorophore, which are located at the opposite ends of the MB, into close proximity, thus effectively quenching the fluorescence (OFF state). Upon hybridization to the target mRNA, the MB in MBMFs undergoes a conformational change that opens the hairpin structure, physically separating the fluorophore from the quencher and allowing fluorescence to be emitted upon excitation (ON state). In addition, the hybridization of MBMFs to the target mRNA can specifically inhibit gene expression through different mechanisms, including translational arrest by steric hindrance of ribosomal activity and the induction of RNase H endonuclease activity,[18] leading to the suppression of cancer cell growth.

L-MBs with the illustrated structure (Figure 1 a) were prepared by directly coupling a diacyllipid phosphoramidite onto the 5′-end of MBs using a fully automated DNA/RNA synthesizer, purified by reversed-phase high-pressure liquid chromatography (HPLC; Supporting Information, Figure S1 a,b), and characterized by ESI-MSn (Figure S1c). The diacyllipid phosphoramidite was synthesized through a three-step reaction according to our previously published proce-

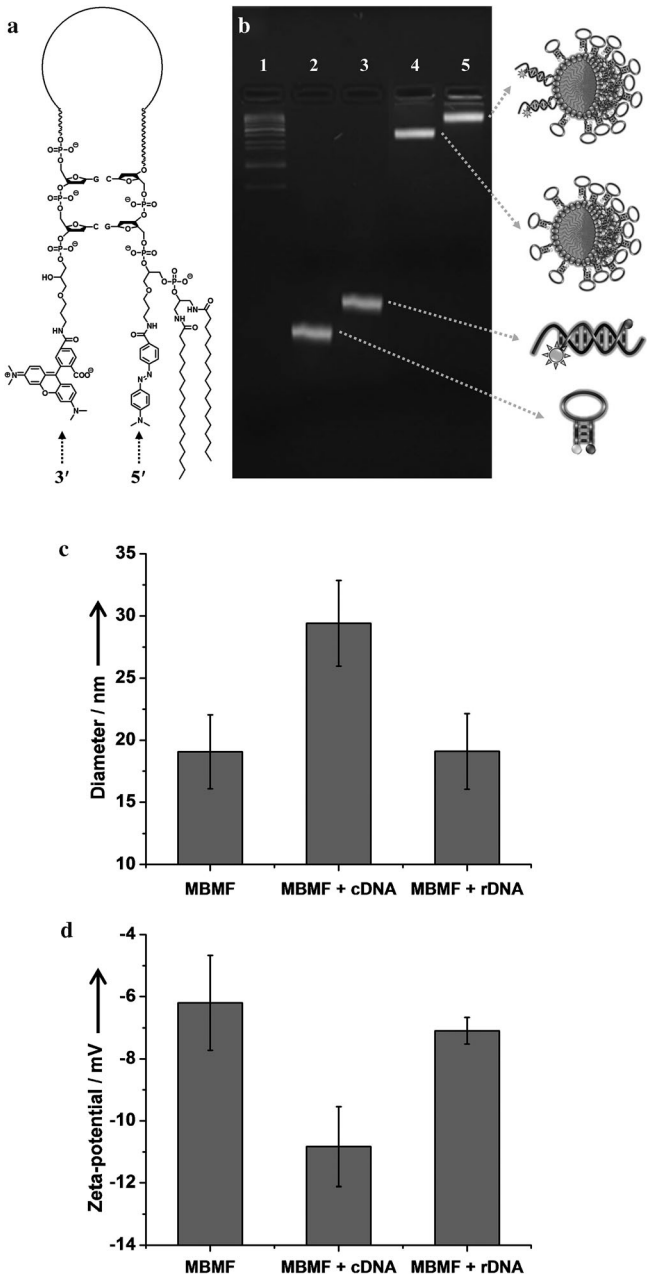

Figure 1. Characterization of MBMFs. a) Structure of MBMFs. Note: not all the bases are shown. b) Agarose gel electrophoresis of DNA marker (lane 1), MBs (lane 2), MBs with synthetic complementary target (cDNA; lane 3), MBMFs (lane 4), and MBMFs with cDNA (lane 5). c) DLS and d) zeta-potential measurements of MBMFs, MBMFs with cDNA, and MBMFs with a synthetic non-complementary target (rDNA).

dure.[19] After purification, L-MBs spontaneously form MBMFs in aqueous solution with a very low critical micelle concentration (CMC; below 10 nM, Figure S2), indicating their excellent stability compared to polymer-micelle systems.[20] The formation of MBMFs was further confirmed by both agarose gel electrophoresis (Figure 1 b) and dynamic light scattering (DLS; Figure 1 c). MBMFs migrated much slower than MBs without diacyllipid, suggesting the successful formation of larger micelle nanostructures. DLS measure-

ments showed that MBMFs had a diameter of 17.1 nm. After adding a synthetic complementary target (cDNA), the diameter increased to 29.4 nm, while incubating MBMFs with a synthetic random control (rDNA) resulted in negligible size increase. Detailed size distribution information can be obtained from the Supporting Information (Figure S3). These results indicated that MBMFs maintained target-recognition capability after the formation of a micellar structure and that the binding event did not disrupt the structural integrity of the micelle. Consistent results were also obtained from zeta-potential measurements: values of −6.2, −10.8, and −7.1 mV were obtained for MBMFs only, MBMFs treated with cDNA, and MBMFs treated with rDNA, respectively (Figure 1d). Detailed sequence information for all the probes used can be found in the Supporting Information (Table S1).

The performance of the MBMFs was first evaluated in a buffer system (see Supporting Information for detailed buffer components and concentration). According to fluorescence spectroscopy results, the response of the MBMFs was specific to the target sequences added, with approximately tenfold signal increase for cDNA, which is much higher than previously mentioned AuNP-nucleic acid conjugates,[5b,17,21] but only minimal signal enhancement when rDNA was added (Figure 2a). In addition, MBMFs were able to differentiate between a perfectly complementary target and mismatched targets (Figure 2b). The fluorescence signal of MBMFs exhibited dose-dependent increases in response to cDNA concentrations from 0 to 1 μM (Figure 2c and Figure S4) with a wide dynamic range from 0 to 200 nM (Figure 2c, Inset). These results demonstrate that MBMFs can effectively signal the presence of a target sequence with excellent selectivity and sensitivity. To compare the stability of MBMFs and MBs towards enzymatic digestion, we incubated each with the endonuclease DNase I (1 U mL^{-1}, significantly greater than what would be found in the cellular environment) and monitored the fluorescence signal increase as a function of time. This experiment showed a much slower increase in fluorescence signal for MBMFs compared to MBs, indicating their enhanced stability owing to increased resistance to enzymatic digestion (Figure 2d). A similar phenomenon was also observed for MBMFs and MBs in cell lysate (Figure S5).

After testing the feasibility of the MBMF approach with a synthetic target, the ability of MBMFs to permeate the cell membrane and detect target mRNA was further investigated. The loop region of L-MBs was designed to be perfectly complementary to *c-raf-1* mRNA, a cancer biomarker and antisense therapeutic target of great significance in cancer diagnostics and theranostics. Non-complementary MBMFs with a similar background signal, but little response to the target (Figure S6), were used as controls. A549 cells were used to verify the ability of MBMFs to detect intracellular mRNA in cancer cells. These adenocarcinoma human alveolar basal epithelial cells come from cancerous lung tissue and have a high expression level of *c-raf-1* mRNA.[5a]

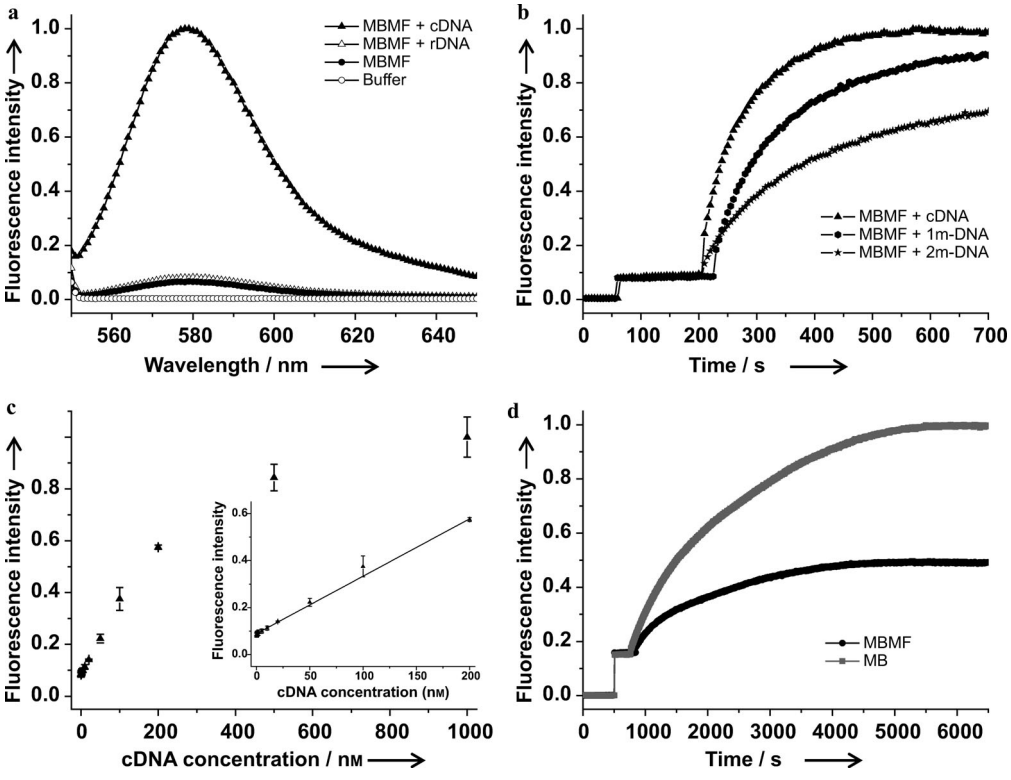

Figure 2. Performance evaluation of MBMFs in a buffer system. a) Fluorescence emission spectroscopy of MBMFs treated with cDNA and rDNA. b) Fluorescence kinetics spectroscopy of MBMFs treated with cDNA, synthetic one-base-mismatch target (1m-DNA), and synthetic two-base-mismatch target (2m-DNA). c) Response of MBMFs to cDNA with concentrations ranging from 0 to 1 μM. Inset: Response of MBMFs to cDNA with concentrations ranging from 0 to 200 nM with an excellent linear relationship. d) Fluorescence kinetics spectroscopy of MBMFs and MBs treated with DNase I.

To obtain optimal results for intracellular detection of *c-raf-1* mRNA, we optimized both the probe concentration and the incubation time for all cell experiments. A549 cells cultured on coverglass-bottom confocal dishes were incubated with 150, 300, and 600 nM MBMFs and then imaged under a confocal laser scanning microscope. Increasing fluorescence signal was observed for cells treated with increasing concentrations of MBMFs (Figure S7). We noticed that the cells treated with 150 nM MBMFs did not generate sufficient fluorescence signal to illuminate *c-raf-1* mRNA, while the cells treated with 600 nM MBMFs resulted in a poor signal-to-background (S/B) ratio. There-

fore, the optimal probe concentration was 300 nM, which had the best combined fluorescence signal and S/B ratio. We also studied the influence of incubation time on the fluorescence signal by incubating A549 cells with 300 nM MBMFs for two or four hours. Because similar fluorescence intensity was observed for both times (data not shown), two hours was chosen as the assay time for the remaining cell experiments. In addition, a co-localization assay demonstrated that most of the fluorescence came from the cytoplasm, instead of the endosomes or lysosomes (Figure S8), indicating that the signal was caused by the specific binding of MBMFs to *c-raf-1* mRNA.

Under optimized conditions, confocal laser scanning microscopy results revealed that A549 cells treated with MBMFs (Figure 3a) displayed much more fluorescence than the population treated with a non-complementary control (Figure 3b) or MBs alone (Figure 3c), demonstrating the selectivity of the system and the need for the diacyllipid moiety for efficient self-delivery. In comparison, a normal bronchial epithelial cell line HBE135 from healthy lung tissue, which expresses significantly less *c-raf-1* mRNA,[22] displayed very low fluorescence (Figure S9). We also used flow cytometry to collect fluorescence data for cells treated with MBMFs. Compared to confocal laser scanning microscopy, which allows imaging of only a small number of cells, flow cytometry can analyze thousands of cells per second, generating a quantifiable statistical average for a large population of cells, while eliminating cell-to-cell variation and experimental artifacts. The flow cytometry results were in excellent agreement with the confocal imaging: 2.61- and 1.08-times signal enhancement were observed for A549 and HBE135 cells, respectively, when incubated with complementary MBMFs (Figure 3b). Thus, while MBMFs work for synthetic target detection in our buffer system, these results also demonstrate that MBMFs are useful for intracellular mRNA detection in living cells. In addition, the MBMF approach can also differentiate cell lines with distinct mRNA expression levels, such as the cancerous and normal cells used here.

Before they can be used for gene therapy, MBMFs must first hybridize with the mRNA. The probe then acts either by blocking translation of the targeted mRNA or by forming a DNA/RNA hybrid with the target mRNA, which can be degraded by the enzyme RNase H.[18] Using these mechanisms, the MBMFs can be used for imaging guided gene therapy.[14a] For this purpose, we used *Raf* genes, which code for serine/threonine-specific protein kinases that play pivotal regulatory roles in the development and maintenance of certain human malignancies. Substantial evidence supports the theory that antisense oligonucleotides targeted against *c-raf-1* kinase can specifically inhibit *c-raf-1* mRNA expression and tumor progression through the aforementioned mechanisms when properly delivered. Therefore, we also tested the anti-proliferative effect of MBMFs on cancer cells. Because gene therapy based on antisense oligonucleotides requires a long treatment period, phosphorothioate MBMFs (S-MBMFs) were used to avoid any potential nuclease digestion in living cells that would diminish the therapeutic efficiency. Experiments showed that this DNA backbone modification

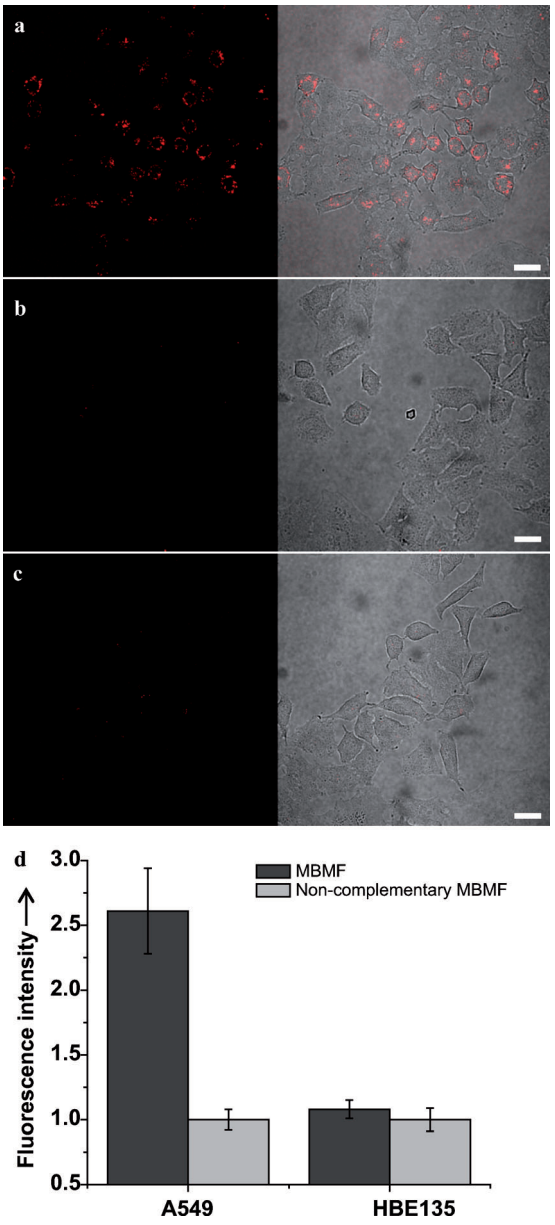

Figure 3. Investigation of MBMFs in living cells. Confocal laser scanning microscopy images of A549 cells treated with 300 nM a) MBMFs, b) non-complementary MBMFs, and c) MBs. Left panels are TAMRA fluorescence pseudo-colored red, and right panels are the overlay of TAMRA fluorescence and the bright-field image. Scale bars = 20 μm. d) Flow cytometry results from A549 and HBE135 cells treated with 300 nM MBMFs and non-complementary MBMFs.

did not significantly affect the performance of S-MBMFs compared to MBMFs because they showed similar low background fluorescence without target or a non-complementary target and maximal fluorescence with excess target (Figure S10). In addition, the S-MBMFs had a comparable CMC (below 20 nM, Figure S11) as the MBMFs (below 10 nM, Figure S2). According to the cytotoxicity assay (Figure 4), A549 cell growth was negligibly influenced by the treatment of cells with non-complementary S-MBMFs, indicating the superior biocompatibility of our system compared to some metal nanoparticle systems.[17] However, their treatment with

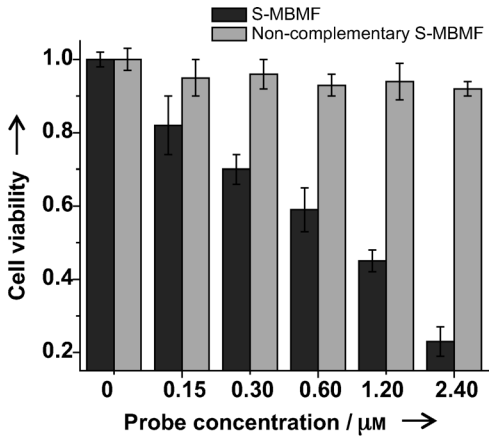

Figure 4. Cytotoxicity assay of A549 cells treated with S-MBMFs and non-complementary S-MBMFs.

S-MBMFs resulted in a marked inhibition of cell proliferation in a dose-dependent manner, suggesting that MBMFs can be applied as an antisense therapy for cancer cells with high expression of *c-raf-1* mRNA.

In summary, we have presented a novel nanoprobe based on molecular assembly that can be used for combined mRNA detection and gene therapy. The advantages of this approach include easy probe synthesis, efficient cellular uptake, enhanced enzymatic stability, high S/B ratio, excellent target selectivity, and superior biocompatibility. Instead of incorporating potentially biohazardous materials for efficient nucleic acid probe delivery, simple modification of MBs with a diacyllipid group provided the resulting MBMFs with new properties that MBs do not have, such as self-delivery and enhanced intracellular stability. In addition to their use in the context of mRNA imaging and gene therapy, MBMFs possess a hydrophobic cavity that could be filled with additional hydrophobic materials, such as magnetic contrast agents or anticancer drugs, showing great promise for constructing an all-in-one nucleic acid probe capable of imaging, diagnosis, and therapy at the same time.

Received: November 26, 2012
Published online: January 14, 2013

Keywords: DNA micelles · gene therapy · mRNA imaging · RNA recognition · self-assembly

[1] a) S. Tyagi, F. R. Kramer, *Nat. Biotechnol.* **1996**, *14*, 303 – 308; b) K. Wang, Z. Tang, C. J. Yang, Y. Kim, X. Fang, W. Li, Y. Wu, C. D. Medley, Z. Cao, J. Li, P. Colon, H. Lin, W. Tan, *Angew. Chem.* **2009**, *121*, 870 – 885; *Angew. Chem. Int. Ed.* **2009**, *48*, 856 – 870.

[2] a) C. Molenaar, S. A. Marras, J. C. M. Slats, J. C. Truffert, M. Lemaitre, A. K. Raap, R. W. Dirks, H. J. Tanke, *Nucleic Acids Res.* **2001**, *29*, 89e; b) K. Okabe, Y. Harada, J. Zhang, H. Tadakuma, T. Tani, T. Funatsu, *Nucleic Acids Res.* **2011**, *39*, e20.

[3] a) S. Tyagi, *Nat. Methods* **2009**, *6*, 331 – 338; b) R. Monroy-Contreras, L. Vaca, *J. Nucleic Acids* **2011**, 741723; c) W. Tan, K. Wang, T. J. Drake, *Curr. Opin. Chem. Biol.* **2004**, *8*, 547 – 553.

[4] H. M. Horton, D. Anderson, P. Hernandez, K. M. Barnhart, J. A. Norman, S. E. Parker, *Proc. Natl. Acad. Sci. USA* **1999**, *96*, 1553 – 1558.

[5] a) B. P. Monia, J. F. Johnston, T. Geiger, M. Muller, D. Fabbro, *Nat. Med.* **1996**, *2*, 668 – 675; b) D. S. Seferos, D. A. Giljohann, H. D. Hill, A. E. Prigodich, C. A. Mirkin, *J. Am. Chem. Soc.* **2007**, *129*, 15477 – 15479.

[6] D. A. Giljohann, D. S. Seferos, A. E. Prigodich, P. C. Patel, C. A. Mirkin, *J. Am. Chem. Soc.* **2009**, *131*, 2072 – 2073.

[7] P. J. Paddison, A. A. Caudy, E. Bernstein, G. J. Hannon, D. S. Conklin, *Genes Dev.* **2002**, *16*, 948 – 958.

[8] L. Hao, P. C. Patel, A. H. Alhasan, D. A. Giljohann, C. A. Mirkin, *Small* **2011**, *7*, 3158 – 3162.

[9] J. Wang, P. C. Zhang, H. Q. Mao, K. W. Leong, *Gene Ther.* **2002**, *9*, 1254 – 1261.

[10] F. S. Du, Y. Wang, R. Zhang, Z. C. Li, *Soft Matter* **2010**, *6*, 835 – 848.

[11] Y. Wu, C. J. Yang, L. L. Moroz, W. Tan, *Anal. Chem.* **2008**, *80*, 3025 – 3028.

[12] a) X. H. Peng, Z. H. Cao, J. T. Xia, G. W. Carlson, M. M. Lewis, W. C. Wood, L. Yang, *Cancer Res.* **2005**, *65*, 1909 – 1917; b) X. Liu, W. Tan, *Anal. Chem.* **1999**, *71*, 5054 – 5059.

[13] a) F. K. Askari, W. M. McDonnell, *N. Engl. J. Med.* **1996**, *334*, 316 – 318; b) R. A. Smith, T. M. Miller, K. Yamanaka, B. P. Monia, T. P. Condon, G. Hung, C. S. Lobsiger, C. M. Ward, M. McAlonis-Downes, H. Wei, E. V. Wancewicz, C. F. Bennett, D. W. Cleveland, *J. Clin. Invest.* **2006**, *116*, 2290 – 2296.

[14] a) G. Liu, M. Swierczewska, S. Lee, X. Chen, *Nano Today* **2010**, *5*, 524 – 539; b) H. Wang, X. Chen, *Expert Opin. Drug Delivery* **2009**, *6*, 745 – 768.

[15] P. C. Patel, D. A. Giljohann, W. L. Daniel, D. Zheng, A. E. Prigodich, C. A. Mirkin, *Bioconjugate Chem.* **2010**, *21*, 2250 – 2256.

[16] D. S. Seferos, A. E. Prigodich, D. A. Giljohann, P. C. Patel, C. A. Mirkin, *Nano Lett.* **2009**, *9*, 308 – 311.

[17] A. Jayagopal, K. C. Halfpenny, J. W. Perez, D. W. Wright, *J. Am. Chem. Soc.* **2010**, *132*, 9789 – 9796.

[18] M. Elsabahy, A. Nazarali, M. Foldvari, *Curr. Drug Delivery* **2011**, *8*, 235 – 244.

[19] a) H. Liu, Z. Zhu, H. Kang, Y. Wu, K. Sefan, W. Tan, *Chem. Eur. J.* **2010**, *16*, 3791 – 3797; b) Y. Wu, K. Sefan, H. Liu, R. Wang, W. Tan, *Proc. Natl. Acad. Sci. USA* **2010**, *107*, 5 – 10.

[20] A. N. Lukyanov, Z. Gao, L. Mazzola, V. P. Torchilin, *Pharm. Res.* **2002**, *19*, 1424 – 1429.

[21] N. Li, C. Chang, W. Pan, B. Tang, *Angew. Chem.* **2012**, *124*, 7544 – 7548; *Angew. Chem. Int. Ed.* **2012**, *51*, 7426 – 7430.

[22] U. R. Rapp, S. M. Storm, J. L. Cleveland in *Modern Trends in Human Leukemia VII*, *Vol. 36*, Springer, Berlin, **1987**, pp. 450 – 459.

